Ecotoxicology and Environmental Safety 207 (2021) 111290

Contents lists available at ScienceDirect

Ecotoxicology and Environmental Safety

journal homepage: www.elsevier.com/locate/ecoenv

The toxic effects and possible mechanisms of decabromodiphenyl ethane on mouse oocyte

Feifei Shi [a,1], Jinyu Qiu [b,1], Jingwen Zhang [a], Sijie Wang [a], Xin Zhao [b,**], Xizeng Feng [a,*]

[a] The Key Laboratory of Bioactive Materials, Ministry of Education, State Key Laboratory of Medicinal Chemical Biology, College of Life Science, Nankai University, Tianjin, 300071, China
[b] The Institute of Robotics and Automatic Information Systems, Nankai University, Tianjin, 300071, China

ARTICLE INFO

Keywords:
Decabromodiphenyl ethane
Oocyte
Mitochondrion
Oxidative stress
Autophagy
Apoptosis

ABSTRACT

Decabromodiphenyl ethane (DBDPE), a widely used new brominated flame retardant, is added into flammable materials to achieve fire retardation. As it is continuously detected in the environment, it has become an emerging environmental pollutant. However, the effects of DBDPE exposure on oocyte maturation and its underlying mechanisms remain unknown. This study found that DBDPE exposure inhibited the rate of germinal vesicle breakdown (GVBD), first polar body extrusion (PBE) and fertilization of mouse oocytes. After 14 h of exposure to DBDPE, metaphase II (MII) oocytes showed that the hardness of zona pellucida (ZP) markedly increased and that the spindle morphology was abnormal. Moreover, DBDPE exposure induced abnormal mitochondrial distribution, mitochondrial dysfunction, and ATP deficiency. Simultaneously, DBDPE exposure down-regulated the expression of antioxidant-related genes (*Sod2*, *Gpx1*) and increased the level of reactive oxygen species (ROS) in oocytes. The results of immunofluorescence and qRT-PCR revealed that autophagy occurred in DBDPE-treated oocytes with high expression of autophagy-related protein (LC3) and genes (*Lc3*, *Beclin1*). Meanwhile, DBDPE significantly up-regulated the protein (Bax) and mRNA (*Bax*, *Caspase3*) levels of pro-apoptosis genes. However, the protein and mRNA expression of anti-apoptosis genes *Bcl-2* was dramatically down-regulated in DBDPE-exposed oocytes. Collectively, DBDPE exposure impaired mitochondrial function, causing oxidative damage, autophagy and apoptosis in oocytes.

1. Introduction

Decabromodiphenyl ethane (DBDPE) is presently used worldwide as a brominated flame retardant (Wang et al., 2019a). Because of excellent flame retardant properties, DBDPE is extensively added to plastic, electronic products, furniture, building materials, textiles, children's toys and other flammable products (Kalachova et al., 2012). Although the global annual output of DBDPE has reached hundreds of thousands of tons, its production and use are still growing rapidly (Besis et al., 2017). In China, DBDPE has become the most widely used flame retardant, and the annual output of DBDPE has reached 31,000 tons in 2016 (Shen et al., 2019). It may release to the surrounding environment continuously from products because DBDPE does not chemically bind to the host substance, which caused the ubiquitous occurrence of DBDPE in the environment (Chen et al., 2019). DBDPE has been detected in a variety of environmental samples, including dust, air (de la Torre et al., 2018; Liu et al., 2016), water (Moller et al., 2011; Zhang et al., 2015), soil sediment (Hu et al., 2010), and sludge (Venkatesan and Halden, 2014). In addition, DBDPE was also detected in human food (aquatic food, egg/egg products) (Shi et al., 2016). The widespread distribution of DBDPE suggests that everyone may be exposed to DBDPE daily, and easily intake DBDPE by eating, drinking and breathing. DBDPE has been detected in human blood, fish, birds and other organisms (Chen et al., 2019; He et al., 2012). More seriously, the research showed that DBDPE is bioaccumulative (Zheng et al., 2014), which may lead to the increasing accumulation of DBDPE in human and other organisms.

Therefore, a comprehensive study on the toxicity of DBDPE is urgent. Four (4) studies have been proved that DBDPE is a thyroid hormone

* Corresponding author. The Key Laboratory of Bioactive Materials, Ministry of Education, State Key Laboratory of Medicinal Chemical Biology, College of Life Science, Nankai University, 94 Weijin Road, Tianjin, 300071, China.
** Corresponding author.
E-mail addresses: zhaoxin@nankai.edu.cn (X. Zhao), xzfeng@nankai.edu.cn (X. Feng).
[1] These authors contributed equally to this study.

https://doi.org/10.1016/j.ecoenv.2020.111290
Received 16 March 2020; Received in revised form 27 July 2020; Accepted 3 September 2020
Available online 15 September 2020

disruptor, as DBDPE exposure altered the levels of thyroid-stimulating hormone (TSH), total thyroxine (TT4) and total triiodothyronine (TT3) (Chen et al., 2019; Smythe et al., 2017; Wang et al., 2019a, 2019b). In another study, DBDPE was reported to be neurotoxic to zebrafish (Jin et al., 2018). Moreover, DBDPE induced oxidative stress and eventually damaged cardiovascular functionality in Sprague-Dawley rats (Jing et al., 2019). DBDPE has been shown to damage the liver function of rats (Sun et al., 2019). However, little is known about the toxic effects of DBDPE on female reproduction.

Oocyte meiotic maturation and the quality of metaphase II (MII) oocytes are two key factors affecting pregnancy outcomes. Germinal vesicle (GV) oocytes undergo germinal vesicle breakdown (GVBD) and first polar body exhaustion (PBE) to complete meiotic maturation. Thus, GVBD and PBE are signs of oocyte meiotic maturation. Even if the oocytes complete meiotic maturation and reach MII oocytes (mature oocyte), fertilization may not be successfully completed, as the quality of MII oocytes is also affected by the mechanical properties of the zona pellucida (ZP) (Yanez et al., 2016), spindle assembly (Howe and Fitz-Harris, 2013), and mitochondrial function (Babayev and Seli, 2015). In addition, it is noteworthy that defects in oocyte quality have been increasing in recent years, and it has been suggested that these adverse phenomena may be related to exposure to certain environmental pollutants (Kramer, 2003; Silbergeld and Patrick, 2005; Stillerman et al., 2008). Therefore, in this study, the hypothesis that DBDPE may be toxic to meiotic maturation or quality of oocytes was proposed.

To test the hypothesis, GV oocytes of mice were exposed to M16 medium containing different concentrations of DBDPE. The effect of DBDPE on oocyte meiotic maturation was evaluated by measuring the ratio of GVBD, PBE, and fertilization. The effect of DBDPE on MII oocyte quality was investigated by detecting mechanical properties, mitochondrial function, spindle assembly, and ROS level. Furthermore, the effects of DBDPE on oocyte autophagy and apoptosis were assessed.

2. Materials and methods

2.1. Chemicals and reagents

DBDPE (certificated standard > 96% pure) was sourced from Yuanye Biotechnology Co., Ltd (Shanghai, China). Pregnant mare serum gonadotropin (PMSG) was obtained from (Ningbo Sansheng Pharmaceutical Co, Ltd. (Ningbo, China). M2 medium and M16 medium were sourced from Sigma-Aldrich (Saint Louis, MO, USA). HTF medium was sourced from Nanjing Aibei Biotechnology Co., Ltd (Nanjing, China). Rabbit polyclonal anti-b-actin, anti-LC3A/B (light chain 3, LC3) antibodies, Mito Tracker Red were obtained from Cell Signaling Technology (MO, USA). Mouse monoclonal anti-BAX, anti-a-tubulin, anti-Bcl2 antibodies were brought from Santa Cruz Biotechnology (Dallas, TX, USA). The dichlorofluorescein diacetate (DCFHDA) and JC-1 were obtained from Beyotime Institute of Biotechnology (Jiangsu, China). DAPI Fluoromount-G was obtained from SouthernBiotech (Birmingham, AL, USA). Other unspecified reagents were sourced from Sigma-Aldrich (Saint Louis, MO, USA).

2.2. Animals, oocyte collection, oocyte treatment and In vitro fertilization (IVF)

6–8 week old female Kunming mice and 12 week old male Kunming mice were sourced from the Institute of Zoology, Chinese Academy of Sciences. All mice were kept in a room with the temperature controlled at 23 ± 2 °C under a 12:12 light/dark cycle (light on at 07:00 a.m.), and free access to food and water. All experimental animal protocols and procedures were approved by the Animal Experimental Committee of the Nankai University (No. 2008) and were performed in accordance with the NIH Guide for the Care and Use of Laboratory Animals. To obtain GV oocytes, female mice were injected with 5 IU of PMSG 48 h prior to being euthanized by cervical dislocation and collection of ovaries. Follicles were punctured with a syringe to obtain GV oocytes.

To test the effect of DBDPE on oocyte maturation, a total of 1986 GV oocytes were randomly divided into the drops of M16 medium with different concentrations of DBDPE (0, 10 μM, 20 μM, 50 μM, 100 μM) (Sun et al., 2012). 30–50 oocytes were placed into one drop of 50 μL M16, covered with mineral oil, and cultured in an incubator (5% CO_2, 37.5 °C, and 100% humidity). The rate of GVBD and PBE were recorded after 2 h and 14 h of culture, respectively. DBDPE was dissolved into dimethyl sulfoxide (DMSO), with a dilution concentration of DMSO being less than one thousandth.

In order to test the effect of DBDPE on the quality of MII oocytes, a total of 600 MII oocytes were used to IVF. Spermatozoa were collected from the cauda epididymidis of male mice and immediately placed in 400 μL warm HTF medium. Then, spermatozoa were capacitated in the incubator (5% CO2, 37.5 °C, and 100% humidity) for 1 h. Spermatozoa (2×10^6 mL^{-1}) were added into the drop of 30 μL HTF medium containing 30 DBDPE-exposed MII oocytes. After 10 h of fertilization, fertilization rates were recorded (oocytes with two pronuclei or two polar bodies were determined to be fertilized oocytes) (Kaneko et al., 2019).

2.3. Measurement of mechanical parameters of MII oocytes

In order to detect the changes of mechanical properties of ZP of MII oocytes after DBDPE exposure, a micro-operating robot system (Fig. S3) was used. To acquire the images of aspiration, the computer controlled the micropipette (outside diameter 28 μm; internal diameter: 25.2 μm) close to the oocyte placed in a 35 mm Petri dish (Falcon, Franklin Lakes, NJ). The ZP of oocyte was inhaled into the micropipette, whilst the aspiration pressure values and the pictures of the elongation of ZP in the micropipette were collected. To estimate the elastic modulus of ZP of oocytes, the current universal shell model was used (Alexopoulos et al., 2005). According to this model, the Young's modulus E of the ZP can be obtained from the following formula:

$$E = 2C(h^*)\left(1-\nu^2\right)\left(\frac{\Delta P}{\Delta L/Rp}\right)$$

where, h^* is the dimensionless thickness of oocyte, which is defined as the ratio of ZP thickness (h) to micropipette radius (Rp); ν, assuming incompressibility ($\nu = 0.5$), was evaluated. C is a function of h^*, which can be expressed by the following formula according to reference (Khalilian et al., 2010).

$$C(h*) = \begin{cases} \dfrac{a + cln(h^*) + eln^2(h^*) + gln^3(h^*) + iln^4(h^*)}{1 + bln(h^*) + dln^2(h^*) + fln^3(h^*) + hln^4(h^*) + jln^5(h^*)} & 0.1 \le (h^*) \le 50 \\ 0.64395655 & (h^*) \ge 50 \end{cases}$$

$a = 1.070275412$, $b = 0.592405186$, $c = -0.44373788$, $d = 0.126723221$, $e = 0.721290633$

$f = 0.074985305$, $g = -0.14390482$, $h = 0.027220129$, $i = 0.040156098$, $j = 0.00132358$.

2.4. Mitochondrial distribution and function analysis

2.4.1. Mitochondrial staining

To monitor the number and distribution of mitochondria in oocytes, a total of 67 MII oocytes (33 oocytes in the control; 34 oocytes in the 50 μM DBDPE group) were dyed in 200 nM Mito Tracker Red CMXRos in M16 medium for 20 min in the dark. After washing three (3) times with PBS, the oocytes were fixed with 4% paraformaldehyde for 1 h and penetrated with membrane permeabilization solution containing 0.5% Triton X-100 for 20 min. Then the oocytes were washed three (3) times and stained with DAPI Fluoromount-G. The red fluorescence was measured by confocal laser-scanning microscope (LSM710, Carl Zeiss, Oberkochen, Germany).

2.4.2. Mitochondrial membrane potential detection

According to the previous method (Marei et al., 2017; Niu et al., 2020; Zand et al., 2018), JC-1 probe was used to detect the mitochondria membrane potential (MMP). Briefly, a total of 34 MII oocytes (16 oocytes in the control; 18 oocytes in the 50 μM DBDPE group) were treated with 1 x JC-1 probe at 37 °C for 20 min in the dark, then washed three (3) times with JC-1 buffer. The fluorescent images were captured using fluorescence microscope (Nikon, Japan). MMP was quantified as the ratio of red to green fluorescence using the Image J software (Version 1.40, National Institutes of Health, Bethesda, MD).

2.4.3. ATP assessment

ATP relative level was evaluated using the ATP Assay Kit. According to the method, 200 MII oocytes from the control group or DBDPE-exposed group were lysed in lysate on ice for 25 min, and centrifuged. The supernatant was used to detect the concentration of ATP. According to the standard curve, ATP concentration was calculated in the control group and DBDPE-exposed group.

2.5. ROS determination in MII oocytes

To determine levels of ROS, a total of 40 MII oocytes (20 oocytes in the control; 20 oocytes in the 50 μM DBDPE group) were incubated in M16 containing 10 mM dichlorofluorescein diacetate (DCFHDA) for 20 min at 37 °C in the dark and then washed three (3) times with PBS. The green fluorescence was measured using fluorescence microscope (Nikon, Japan).

2.6. Immunofluorescence

In order to detect the spindle and autophagy of MII oocytes, the expression of α-tubulin (36 oocytes were used in the control; 32 oocytes were used in the 50 μM DBDPE group) and LC3 (32 oocytes were used in the control; 32 oocytes were used in the 50 μM DBDPE group) were detected. Briefly, MII oocytes were fixed in 4% paraformaldehyde for 1 h and then permeabilized with 0.5% Triton X-100 for 30 min. Nonspecific binding of antibodies was blocked by 1% BSA/PBS for 1 h at room temperature. Then, MII oocytes were incubated with anti-LC3 antibody or anti-α-tubulin antibody for 2 h at room temperature, washed in PBS three (3) times, subsequently incubated with secondary antibody for 1 h at room temperature. Next, the samples were washed and stained with DAPI Fluoromount-G to visualize nuclei. Finally, the oocytes were examined using confocal laser-scanning microscope (LSM710, Carl Zeiss, Oberkochen, Germany).

2.7. RNA isolation and quantitative real time PCR

200 MII oocytes in the control or in 50 μM DBDPE-treated group were used to extract total RNA using the TRNpure Total RNA Kit (Nobelab, Beijing, China). Total RNA is used to reverse cDNA with PrimeScript RT Reagent Kit (TaKaRa, Dalian, China). Real-time polymerase chain reaction (PCR) was performed using SYBR green master mix on LightCycler 96 System (Roche Diagnostics Ltd, Basel, Switzerland). The sequences of the primers used are presented in Table S1. PCR was performed in triplicate and was presented relative to the abundance of endogenous GAPDH in the same sample. The gene expression levels were computed according to the $2^{-\Delta\Delta Ct}$ method (Jia et al., 2019).

2.8. Western blot

To extract protein, 300 MII oocytes in the control or in 50 μM DBDPE-treated group were lysed with SDS sample buffer containing 1 x protease inhibitor Cocktail (cwbio-tech) on ice for 10 min. Protein samples were then boiled at 100 °C for 5 min, and separated with 12% SDS-PAGE. After electrophoretic separation, separated proteins were electrically transferred into a PVDF membrane (Immobilon-P; Millipore, Bedford, MA). The PVDF membrane with protein was blocked for 2 h with 5% nonfat milk, and incubated with primary antibody for 2 h at room temperature (anti-BAX antibody, 1:500; anti-Bcl2 antibody, 1:1000; anti-β-actin antibody, 1:1000). Washing three (3) times with TBST (5 min each), PVDF membrane were incubated for 1 h with appropriate secondary antibodies. After washing, the protein bands were visualized and the images were quantified using Image J software (Version 1.40, National Institutes of Health, Bethesda, MD).

2.9. Statistical analysis

All data were analyzed using GraphPad Prism 8.0 software. Differences between the two (2) groups (10 μM DBDPE vs Control, 20 μM DBDPE vs Control, 50 μM DBDPE vs Control, and 100 μM DBDPE vs Control) were analyzed by the Student's unpaired two-tailed *t*-test. *P* value < 0.05 was considered statistically significant. In all figures, one (1), two (2), and three (3) asterisks indicate $^{*}p < 0.05$, $^{**}p < 0.01$ and $^{***}p < 0.001$, respectively. Data in bar plots are shown as the mean ± SEM. The boxplot represents the median, the first quartile and the third quartile of values. Experiments were conducted in triplicate.

3. Results

3.1. DBDPE exposure inhibited the maturation and fertilization of mouse oocyte

In order to detect the toxic effect of DBDPE on oocytes, 1968 GV oocytes were used for *in vitro* maturation. Then, the ratio of GVBD and PBE oocytes were recorded in different concentrations of DBDPE (0, 10 μM, 20 μM, 50 μM, 100 μM). Compared with the control group, DBDPE exposure significantly reduced the ratio of GVBD and PBE in a dose-dependent manner (GVBD, control: 84.3 ± 2.3%, 20 μM: 71.3 ± 2.4%, 50 μM: 62.0 ± 3.5%, 100 μM: 55.7 ± 1.8%; PBE, control: 74.3 ± 1.5%, 20 μM: 62.7 ± 1.5%, 50 μM: 51.0 ± 2.0%, 100 μM: 28.0 ± 2.6%, Fig. 1A and B, Fig. S1). The result indicated that DBDPE exposure inhibited oocyte maturation. For subsequent experiments, 50 μM was used as the treatment concentration. Fertilization rate was considered the endpoint of evaluating maturation and quality of oocyte. 600 MII oocytes were used for IVF, and the results showed that the rate of fertilization of MII oocytes exposed to 50 μM DBDPE was significantly lower than that of the control group (77.3 ± 2.9% versus 52.7 ± 2.9%, Fig. 1C, Fig. S2). The representative pictures of the three (3) stages of GVBD, PBE and fertilization were shown in Fig. 1D. Thus, these results indicated that DBDPE exposure affected oocyte maturation and fertilization.

3.2. DBDPE exposure caused ZP to harden in mouse MII oocyte

The hardness of ZP affects the fertilization of oocyte. To investigate whether DBDPE inhibited fertilization by changing the hardness of ZP, the mechanical parameters of ZP of oocytes were measured by the micropipette aspiration technique using a mechanical detection system (Fig. S3). Images of MII oocytes in the control and DBDPE treated group

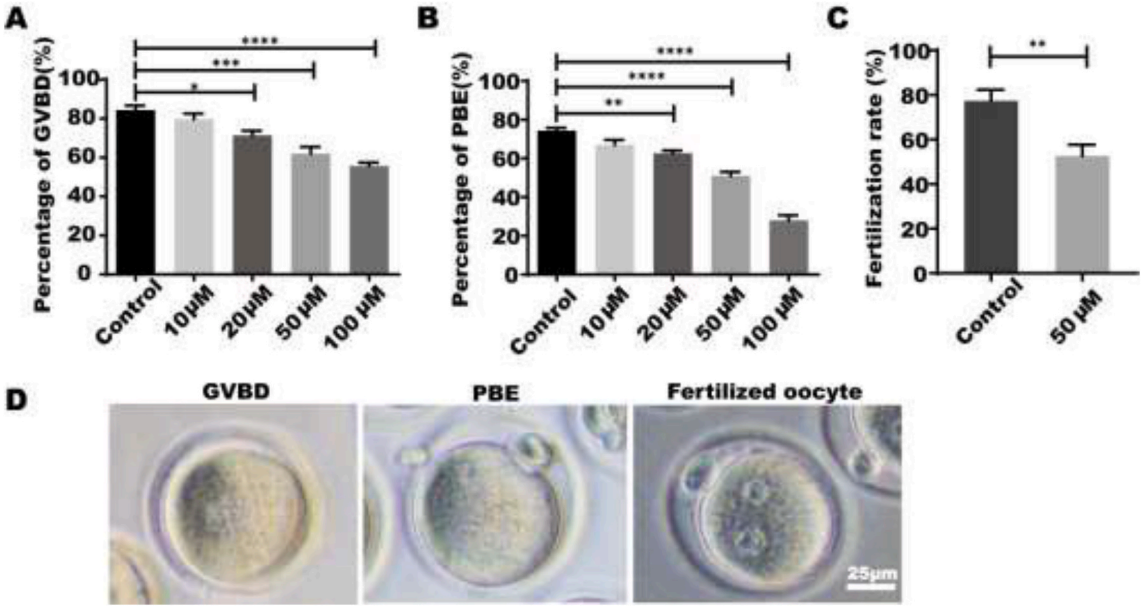

Fig. 1. DBDPE exposure inhibited the maturation and fertilization of mouse oocyte. A, Percentage of germinal vesicle breakdown (GVBD) of oocytes in different DBDPE-exposed groups. B, Percentage of first polar body exhaustion (PBE) of oocytes in different DBDPE-treated groups. C, The rate of fertilization of oocyte in the control and the 50 μM DBDPE-treated group. D, Representative images of oocytes at different development stages (GVBD: germinal vesicle breakdown; PBE: first polar body extrusion). All data were shown as mean ± SEM. $^{*}p < 0.05$, $^{**}p < 0.01$, $^{***}p < 0.001$, $^{****}p < 0.0001$ (Student's unpaired two-tailed *t*-test).

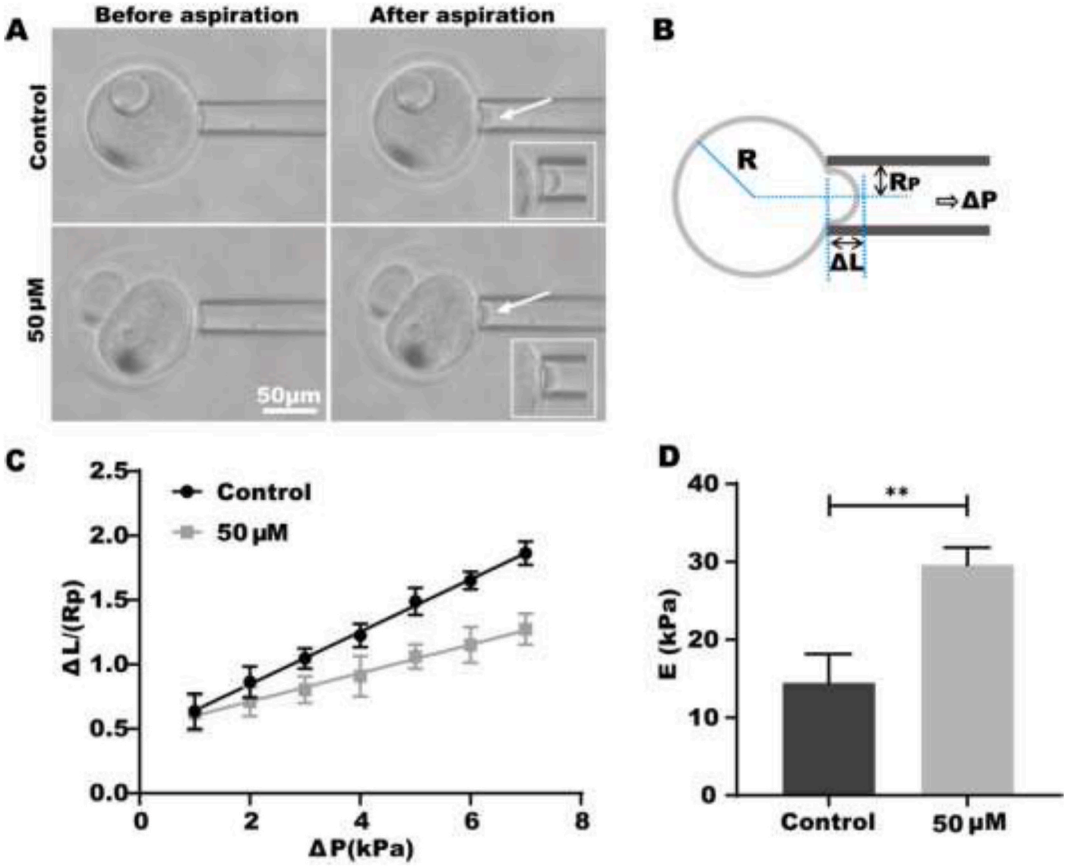

Fig. 2. DBDPE exposure caused ZP to harden in mouse MII oocyte. A, Images of elongation of ZP by micropipette aspiration at the same differential pressure in different groups, white arrows indicated ZP sucked into the micropipette and white box showed partially enlarged image. B, The shell model of oocyte for estimation of Young's modulus; Rp: the radius of micropipette. ΔL: elongation of the ZP sucked into the micropipette, ΔP: pressure difference. C, The relationship between the pressure and elongation of the ZP. D, The Young's modulus of the ZP of oocytes in the control and 50 μM DBDPE-exposed group, data were shown as mean ± SEM. $^{**}p < 0.01$ (Student's unpaired two-tailed *t*-test).

were shown in Fig. 2A, and the results showed that the ZP elongation of 50 μM DBDPE-treated oocytes was lower than that of the control group under the same holding pressure difference. In this experiment, the Young's modulus was used to represent the hardness of the ZP, and the current universal shell model was used to calculate the young's modulus of the ZP (Fig. 2B). The relationship between pressure and ZP elongation was shown in Fig. 2C. The results showed that the Young's modulus of the ZP of the oocytes in the control group was 14.3 ± 2.1 kPa, however, the Young's modulus of the ZP of oocytes was significantly increased (29.5 ± 1.3 kPa) in 50 μM DBDPE treated group ($p < 0.01$, Fig. 2D). Therefore, DBDPE led to ZP hardening, which inhibited the fertilization.

3.3. DBDPE exposure induced mitochondrial dysfunction, and ATP deficiency

Then, to further explore the effect of DBDPE on mitochondria, the mitochondria distribution and function were examined in MII oocytes. The MitoTracker Red was used to label mitochondria in MII oocytes, and the results showed that mitochondria were uniformly distributed among the whole oocyte cytoplasm in the control. However, the mitochondrial distribution was marginalized in the 50 μM DBDPE-exposed oocyte cytoplasm (Fig. 3A). Moreover, it was also observed that the number of mitochondria in oocytes treated with 50 μM DBDPE was lower than that in the control group by MitoTracker Red fluorescence intensity statistics ($p < 0.01$, Fig. 3B). Next, mitochondrial membrane potential (MMP) of MII oocytes was detected by JC-1 (Fig. 3C). The ratio of fluorescence intensity (red/green) decreased significantly in the 50 μM DBDPE-treated group as compared to that in the control group ($p < 0.001$, Fig. 3 D), suggesting that DBDPE exposure resulted in a loss of mitochondrial membrane potential. Moreover, ATP production markedly decreased in the DBDPE-treated oocytes compared with control ($p < 0.0001$, Fig. 3E). Therefore, DBDPE exposure injured the mitochondria, which is the vital factor affecting oocyte maturation and fertilization.

3.4. DBDPE exposure induced oxidative stress and spindle defects in mouse MII oocyte

ROS is a by-product of mitochondria and mitochondrial dysfunction leads to the increase of ROS in cell. ROS in MII oocytes were further evaluated in this study. The ROS fluorescence image of oocytes in the control and 50 μM DBDPE group were shown in Fig. 4A, and the fluorescence intensity of ROS was dramatically higher in the 50 μM DBDPE treatment group than in the control ($p < 0.001$, Fig. 4B). Furthermore, the results of the relative mRNA expression of anti-oxidative genes showed that *Gpx1* and *Sod2* down-regulated in the 50 μM DBDPE treated group (Fig. 4C). The result indicated that DBDPE exposure induced oxidative stress of oocyte. Complete spindle structure is essential for meiosis and fertilization. As shown in Fig. 4D, the MII oocytes showed regular spindle assembly in the control group. However, spindle assembly was disrupted severely in MII oocytes treated with 50 μM DBDPE (Fig. 4D). The abnormal rate of spindle of MII oocytes in 50 μM DBDPE treated group increased (36.5 ± 2.2%), compared with the control group (18.5 ± 3.1%, Fig. 4E).

3.5. DBDPE exposure caused autophagy and apoptosis in mouse MII oocytes

The levels of autophagy and apoptosis in MII oocytes were measured finally, qPCR results showed that compared with the control group, the mRNA expression levels of autophagy-related genes *Lc3*, *Beclin1* significantly increased and the mRNA expression levels of *mTOR* significantly decreased in 50 μM DBDPE-exposed MII oocytes (Fig. 5A). Immunofluorescence results showed that autophagy-related protein LC3 expression increased in the oocytes treated with 50 μM DBDPE (Fig. 5B and C). Moreover, the mRNA levels of pro-apoptosis genes *Caspase3* and *Bax* were markedly up-regulated in DBDPE-treated oocytes than in the control, whereas the relative quantification of anti-apoptosis gene *Bcl-xl* was dramatically down-regulated in DBDPE-treated samples than in controls (Fig. 5D). The Western blot results also suggested that the protein expression level of BAX in the DBDPE-treated group was significantly higher than that in the control group, however, the protein expression level of Bcl2 in the DBDPE-treated group was lower than that in the control group (Fig. 5E and F). The results indicated that DBDPE exposure led to the autophagy and apoptosis of oocyte.

4. Discussion

This study detected the toxic effect of DBDPE exposure on mouse oocyte. The results showed that exposure to DBDPE significantly inhibited oocyte meiotic maturation and resulted in damage to MII oocytes. The potential toxic mechanism of DBDPE is that DBDPE induced mitochondrial disorders, resulting in ATP deficiency and excessive ROS generation. Excessive ROS further caused damage of the spindle and ZP, ultimately leading to oocyte autophagy and apoptosis.

GVBD and PBE are important markers of oocyte meiotic maturation (Reyes and Ross, 2016). The results of this study showed that compared with the control group, the rate of GVBD and PBE of oocytes treated with DBDPE were reduced, which indicated DBDPE was toxic to meiotic maturation of oocytes. The effect of DBDPE on the quality of MII oocytes by IVF was further verified. The results showed that the IVF of MII oocytes exposed to DBDPE decreased markedly, suggesting that DBDPE lead to defects in oocyte quality.

The mechanical properties of oocytes determine the developmental potential of oocytes (Yanez et al., 2016). The change of mechanical properties affects oocytes fertilization. However, little attention has been paid to the changes of mechanical properties of oocytes caused by the compounds. Therefore, the effect of DBDPE exposure on the mechanical properties of ZP was explored and the results found that after DBDPE exposure, the elongation rate of ZP decreased and the Young's modulus markedly increased. These results indicated that DBDPE exposure caused the ZP to harden. Previous studies reported that DBDPE can be embedded in cell membranes, resulting in reduced cell membrane fluidity (Liu et al., 2019). DBDPE may be embedded in the ZP to cause the ZP to harden. Hardened ZP significantly reduced the fertilization ability of oocytes (Wassarman and Litscher, 2018). Therefore, the hardened ZP caused by DBDPE exposure led to the decreased rate of fertilization.

In oocytes, mitochondria are involved in the regulation of ATP production, cytoplasmic redox, signal transduction and apoptosis (Roth, 2018), therefore it was used as a valuable marker to reflect the quality of oocytes (Roth, 2018). After the oocyte maturation, mitochondria migrate from the cortex to the entire cytoplasm, and the number increases (Bavister and Squirrell, 2000; Brevini et al., 2005). Oocytes with more mitochondria have high developmental potential (Van Blerkom and Davis, 2007). The increase of mitochondria produces more ATP and provides the oocytes with enough energy. The decrease of ATP level affected the process of mouse oocyte maturation and preimplantation embryo development (Yu et al., 2010). Reduction of mitochondrial membrane potential also led to failure of oocyte maturation (Lee et al., 2014). In this study, it was observed that DBDPE exposure reduced the number of mitochondria and affected the migration of mitochondria from cortex to cytoplasm. Moreover, both the mitochondrial membrane potential and ATP level decreased obviously in oocytes after DBDPE treatment. Previous study found that DBDPE exposure interfered with thyroid hormone (Chen et al., 2019), and thyroid hormone disorder affected the organization of respiratory chain, oxidative phosphorylation and ATP production, leading to mitochondrial function damage in human pre-implantation embryos (Noli et al., 2020). Therefore, based on previous studies and the results of this study, mitochondrial dysfunction induced by DBDPE exposure is the main factor leading to oocyte toxicity.

Impaired mitochondrial function caused abnormal levels of ROS in

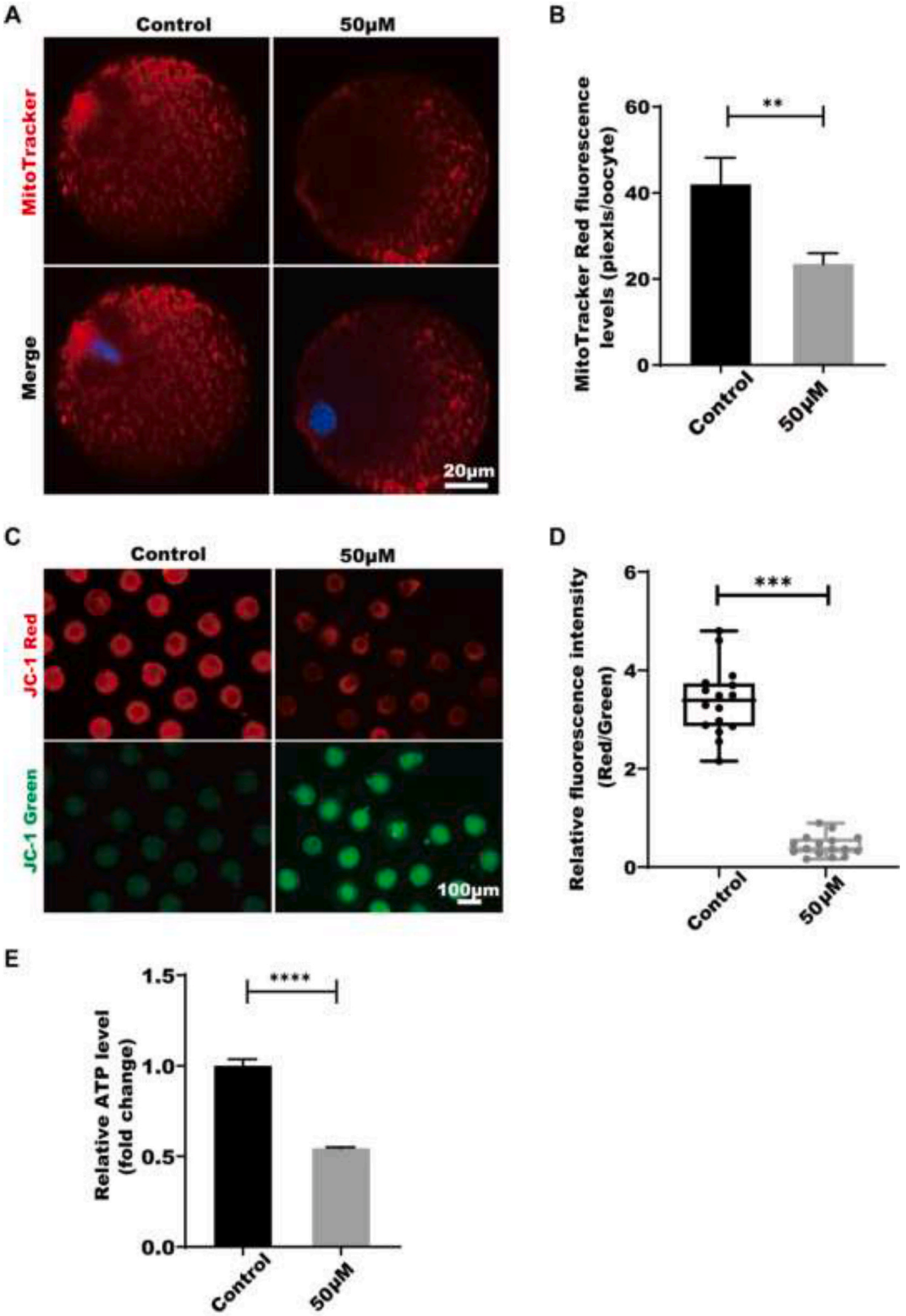

Fig. 3. DBDPE exposure induced mitochondrial dysfunction, and ATP deficiency A, The distribution of mitochondria in MII oocytes. Red: Mitochondrial Tracker; blue, DNA; B, MitoTracker Red fluorescence level of MII oocytes in control group and in 50 μM DBDPE exposure group, data were shown as mean ± SEM, $^{**}p < 0.01$ (Student's unpaired two-tailed *t*-test). C, Representative images of JC-1 staining. D, The fluorescence intensity (red/green) of mitochondrial membrane potential (MMP) of oocytes. The box plots shows median, 25th and 75th percentiles, and whiskers extending to maximum and minimum data points, $^{***}p < 0.001$ (Student's unpaired two-tailed *t*-test). E, ATP levels of MII oocytes in different groups, data were shown as mean ± SEM, $^{****}p < 0.0001$ (Student's unpaired two-tailed *t*-test). (For interpretation of the references to colour in this figure legend, the reader is referred to the Web version of this article.)

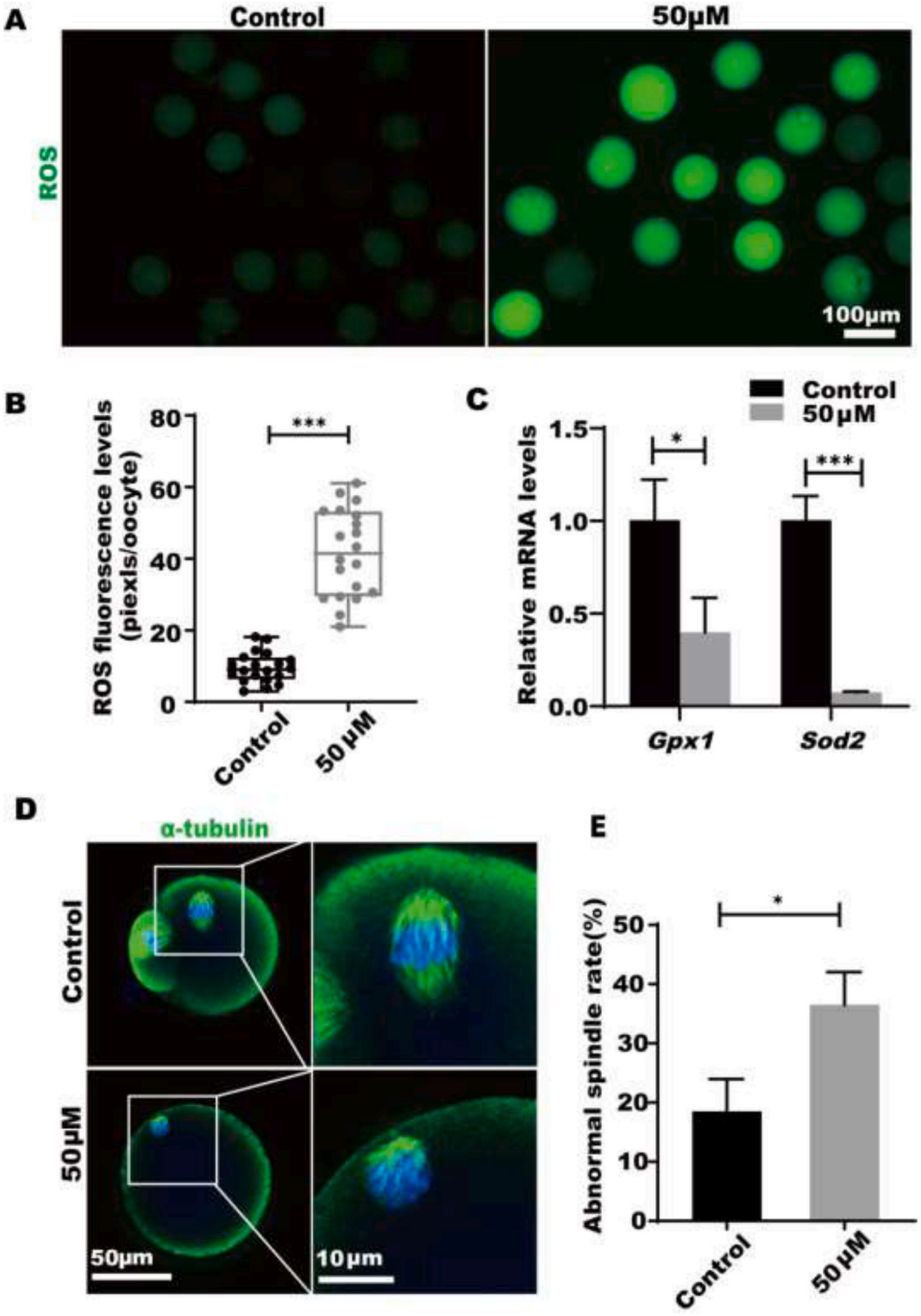

Fig. 4. DBDPE exposure induced oxidative stress and spindle defects in mouse MII oocyte. A, ROS fluorescently stained images. B, Fluorescence intensity quantification in the control and the 50 μM DBDPE exposure group, and the box plots shows median, 25th and 75th percentiles, and whiskers extending to maximum and minimum data points, $^{***}p < 0.001$ (Student's unpaired two-tailed *t*-test). C, Relative mRNA expression of antioxidant related genes, *Gpx1* and *Sod2*, data were shown as mean ± SEM, $^{*}p < 0.05$, $^{***}p < 0.001$ (Student's unpaired two-tailed *t*-test). D, Representative images of spindle in different groups. Green, α-tubulin; blue, DNA; E, The rate of the abnormal spindle in the control and DBDPE-exposed group. Data were shown as mean ± SEM, $^{*}p < 0.05$ (Student's unpaired two-tailed *t*-test). (For interpretation of the references to colour in this figure legend, the reader is referred to the Web version of this article.)

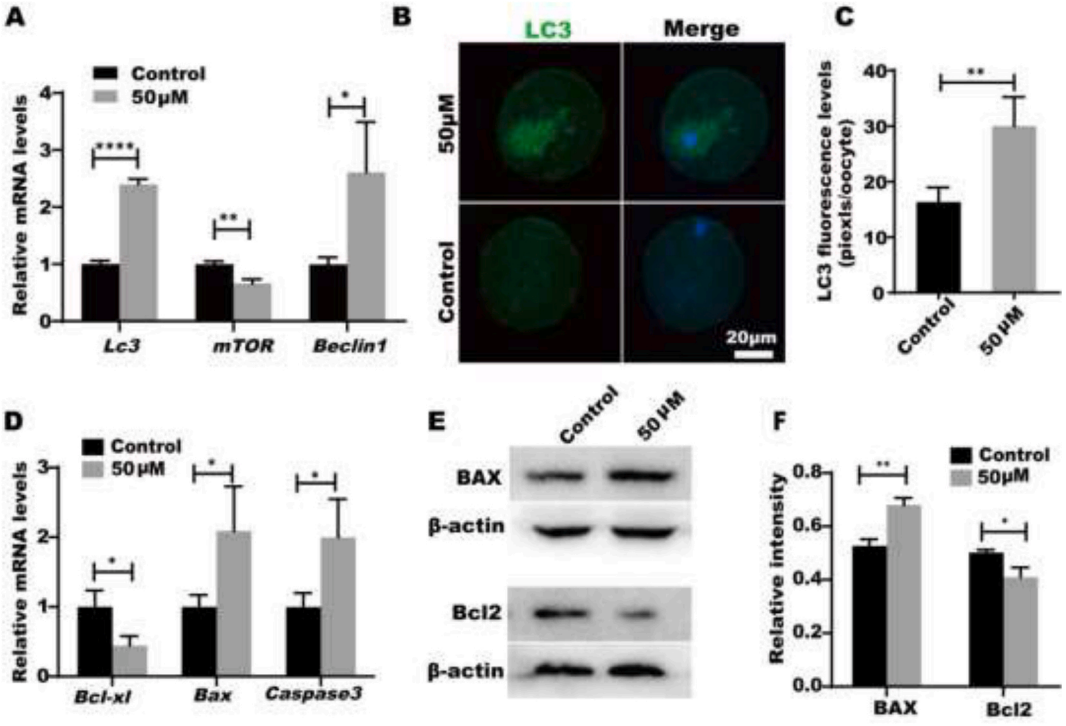

Fig. 5. DBDPE exposure caused autophagy and apoptosis in mouse MII oocytes. A, The mRNA expression of autophagy related genes. B, Immunofluorescence image of LC3 protein in MII oocytes; green: LC3. blue: DAPI. C, Quantification of fluorescence intensity of LC3 protein in the control and the 50 μM DBDPE exposure group. D, The relative mRNA level of apoptotic-related genes in MII oocytes, data were shown as mean ± SEM, $*p < 0.05$, $**p < 0.01$ (Student's unpaired two-tailed *t*-test). E and F, The expression levels of apoptotic-related protein in MII oocytes, data were shown as mean ± SEM, $*p < 0.05$, $**p < 0.01$ (Student's unpaired two-tailed *t*-test). (For interpretation of the references to colour in this figure legend, the reader is referred to the Web version of this article.)

oocytes (Gurung et al., 2015). Consistent with the previous study (Gurung et al., 2015), the results of this study showed a significant increase of ROS in oocytes, with mitochondrial dysfunction caused by DBDPE. In redox homeostasis, antioxidant enzymes can scavenge excessive ROS. However, when the expression of antioxidant enzyme decreased, the level of oxidative stress would be increased (Zhang et al., 2019). The result of qPCR showed antioxidant gene expression of *Sod2* and *Gpx-2* down-regulated after DBDPE exposure, which further caused the production of excessive ROS. Excessive ROS could damage DNA, protein, lipid and other cell components (Filomeni et al., 2015). The results of immunofluorescence showed the structural damage of spindle in MII oocytes after DBDPE exposure. Therefore, excessive ROS induced spindle defect in DBDPE exposed oocyte. Spindle in meiotic cells is responsible for the separation of homologous chromosomes in meiosis I and sister chromatids in meiosis II, spindle assembly errors led to oocyte development retardation and aneuploidy (Howe and FitzHarris, 2013). Moreover, abnormal spindle morphology led to IVF failure and abnormal division (Keefe et al., 2003). Therefore, ROS-induced spindle defect inhibited maturation and fertilization of oocyte treated with DBDPE.

Oxidative stress and other adverse conditions caused oocytes autophagy and apoptosis (Jia et al., 2019). Therefore, the autophagy level after DBDPE exposure was detected. Inhibition of mammalian target of rapamycin (mTOR) induced autophagy (Sarbassov et al., 2005). Beclin1 mediated the formation of proautophagy and recruited microtubule-associated light chain protein (LC3) to promote the expansion of phagocytic vesicles (Han et al., 2016). Thus, LC3, Beclin1, and mTOR are recognized markers of autophagy and the results showed that the mRNA expression of *Lc3*, *Beclin1* up-regulated, the mRNA expression of *mTOR* down-regulated, and the expression of LC3 protein increased in oocytes treated with DBDPE. The results suggested that DBDPE activated the autophagy in oocytes. Moreover, abnormal intracellular signals led to the activation of Bax, inhibited the expression of Bcl-2, induced mitochondria release of cytochrome c, and then led to the occurrence of apoptosis mediated by mitochondria (Wang et al., 2019c). The results of qRT-PCR analysis showed that the expression of *Bax* and *Caspase3* increased and the expression of *Bcl-xl* decreased in DBDPE-treated oocytes. By Western blot analysis, the results showed that the protein expression of Bax increased and the protein expression of Bcl-2 decreased. Thus, DBDPE exposure induced autophagy and apoptosis.

5. Conclusion

In summary, this study confirmed that DBDPE exposure inhibited maturation and fertilization of mouse oocyte, therefore DBDPE is toxic for the development of mouse oocyte. The possible mechanism of toxicity is that DBDPE interferes with mitochondrial function, which leads to ATP deficiency and excessive production of ROS. Excessive ROS leads to the damage of ZP and spindle, finally inducing autophagy and apoptosis of oocytes. This study provides evidence and potential mechanism for DBDPE toxicity in oocytes.

Author contributions

X.Z.F., and F.F.S., conceived and designed the experiments. F.F.S., J. Y.Q and J.W.Z. conducted the experiments and data analysis. S.J.W. conducted gene expression analysis. F.F.S. wrote the manuscript.

Declaration of competing interest

The authors declare that they have no known competing financial interests or personal relationships that could have appeared to influence the work reported in this paper.

Acknowledgments

This project was initiated in the Key Laboratory of Bioactive Materials, Ministry of Education, at Nankai University. This work was supported by the Special Fund for Basic Research on Scientific Instruments of the Chinese National Natural Science Foundation [grant no: 61327802, U1613220].

Appendix A. Supplementary data

Supplementary data to this article can be found online at https://doi.org/10.1016/j.ecoenv.2020.111290.

References

Alexopoulos, L.G., et al., 2005. The biomechanical role of the chondrocyte pericellular matrix in articular cartilage. Acta Biomater. 1, 317–325.
Babayev, E., Seli, E., 2015. Oocyte mitochondrial function and reproduction. Curr. Opin. Obstet. Gynecol. 27, 175–181.
Bavister, B.D., Squirrell, J.M., 2000. Mitochondrial distribution and function in oocytes and early embryos. Hum. Reprod. 15 (Suppl. 2), 189–198.
Besis, A., et al., 2017. Legacy and novel brominated flame retardants in interior car dust – implications for human exposure. Environ. Pollut. 230, 871–881.
Brevini, T.A., et al., 2005. Role of adenosine triphosphate, active mitochondria, and microtubules in the acquisition of developmental competence of parthenogenetically activated pig oocytes. Biol. Reprod. 72, 1218–1223.
Chen, T., et al., 2019. Thyroid function and decabromodiphenyl ethane (DBDPE) exposure in Chinese adults from a DBDPE manufacturing area. Environ. Int. 133, 105179.
de la Torre, A., et al., 2018. Traditional and novel halogenated flame retardants in urban ambient air: gas-particle partitioning, size distribution and health implications. Sci. Total Environ. 630, 154–163.
Filomeni, G., et al., 2015. Oxidative stress and autophagy: the clash between damage and metabolic needs. Cell Death Differ. 22, 377–388.
Gurung, P., et al., 2015. Mitochondria: diversity in the regulation of the NLRP3 inflammasome. Trends Mol. Med. 21, 193–201.
Han, J., et al., 2016. Deoxynivalenol exposure induces autophagy/apoptosis and epigenetic modification changes during porcine oocyte maturation. Toxicol. Appl. Pharmacol. 300, 70–76.
He, M.J., et al., 2012. Bioaccumulation of polybrominated diphenyl ethers and decabromodiphenyl ethane in fish from a river system in a highly industrialized area, South China. Sci. Total Environ. 419, 109–115.
Howe, K., FitzHarris, G., 2013. Recent insights into spindle function in mammalian oocytes and early embryos. Biol. Reprod. 89, 71.
Hu, G., et al., 2010. Distribution of polybrominated diphenyl ethers and decabromodiphenylethane in surface sediments from Fuhe River and Baiyangdian Lake, North China. J. Environ. Sci. (China) 22, 1833–1839.
Jia, Z.Z., et al., 2019. Deltamethrin exposure induces oxidative stress and affects meiotic maturation in mouse oocyte. Chemosphere 223, 704–713.
Jin, M.Q., et al., 2018. Neurological responses of embryo-larval zebrafish to short-term sediment exposure to decabromodiphenylethane. J. Zhejiang Univ. - Sci. B 19, 400–408.
Jing, L., et al., 2019. Cardiovascular toxicity of decabrominated diphenyl ethers (BDE-209) and decabromodiphenyl ethane (DBDPE) in rats. Chemosphere 223, 675–685.
Kalachova, K., et al., 2012. Occurrence of brominated flame retardants in household and car dust from the Czech Republic. Sci. Total Environ. 441, 182–193.
Kaneko, H., et al., 2019. Developmental ability of oocytes retrieved from Meishan neonatal ovarian tissue grafted into nude mice. Anim. Sci. J. 90, 344–352.
Keefe, D., et al., 2003. Imaging meiotic spindles by polarization light microscopy: principles and applications to IVF. Reprod. Biomed. Online 7, 24–29.
Khalilian, M., et al., 2010. Estimating Young's modulus of zona pellucida by micropipette aspiration in combination with theoretical models of ovum. J. R. Soc. Interface 7, 687–694.
Kramer, M.S., 2003. The epidemiology of adverse pregnancy outcomes: an overview. J. Nutr. 133, 1592S–1596S.
Lee, S.K., et al., 2014. The association of mitochondrial potential and copy number with pig oocyte maturation and developmental potential. J. Reprod. Dev. 60, 128–135.
Liu, L.Y., et al., 2016. Trends in the levels of halogenated flame retardants in the Great Lakes atmosphere over the period 2005-2013. Environ. Int. 92–93, 442–449.
Liu, Y., et al., 2019. Exploring the membrane toxicity of decabromodiphenyl ethane (DBDPE): based on cell membranes and lipid membranes model. Chemosphere 216, 524–532.
Marei, W.F.A., et al., 2017. Alpha-linolenic acid protects the developmental capacity of bovine cumulus–oocyte complexes matured under lipotoxic conditions in vitro. Biol. Reprod. 96, 1181–1196.
Moller, A., et al., 2011. Polybrominated diphenyl ethers (PBDEs) and alternative brominated flame retardants in air and seawater of the European Arctic. Environ. Pollut. 159, 1577–1583.
Niu, Y., et al., 2020. Melatonin enhances mitochondrial biogenesis and protects against rotenone-induced mitochondrial deficiency in early porcine embryos. J. Pineal Res. 68.
Noli, L., et al., 2020. Effects of thyroid hormone on mitochondria and metabolism of human preimplantation embryos. Stem Cell. 38, 369–381.
Reyes, J.M., Ross, P.J., 2016. Cytoplasmic polyadenylation in mammalian oocyte maturation. Wiley Interdiscip Rev RNA 7, 71–89.
Roth, Z., 2018. Symposium review: reduction in oocyte developmental competence by stress is associated with alterations in mitochondrial function. J. Dairy Sci. 101, 3642–3654.
Sarbassov, D.D., et al., 2005. Growing roles for the mTOR pathway. Curr. Opin. Cell Biol. 17, 596–603.
Shen, K., et al., 2019. Stocks, flows and emissions of DBDPE in China and its international distribution through products and waste. Environ. Pollut. 250, 79–86.
Shi, Z., et al., 2016. Novel brominated flame retardants in food composites and human milk from the Chinese Total Diet Study in 2011: concentrations and a dietary exposure assessment. Environ. Int. 96, 82–90.
Silbergeld, E.K., Patrick, T.E., 2005. Environmental exposures, toxicologic mechanisms, and adverse pregnancy outcomes. Am. J. Obstet. Gynecol. 192, S11–S21.
Smythe, T.A., et al., 2017. Impacts of unregulated novel brominated flame retardants on human liver thyroid deiodination and sulfotransferation. Environ. Sci. Technol. 51, 7245–7253.
Stillerman, K.P., et al., 2008. Environmental exposures and adverse pregnancy outcomes: a review of the science. Reprod. Sci. 15, 631–650.
Sun, R.B., et al., 2012. Cytotoxicity and apoptosis induction in human HepG2 hepatoma cells by decabromodiphenyl ethane. Biomed. Environ. Sci. 25, 495–501.
Sun, Y., et al., 2019. Hepatotoxicity of decabromodiphenyl ethane (DBDPE) and decabromodiphenyl ether (BDE-209) in 28-day exposed Sprague-Dawley rats. Sci. Total Environ. 135783.
Van Blerkom, J., Davis, P., 2007. Mitochondrial signaling and fertilization. Mol. Hum. Reprod. 13, 759–770.
Venkatesan, A.K., Halden, R.U., 2014. Brominated flame retardants in U.S. biosolids from the EPA national sewage sludge survey and chemical persistence in outdoor soil mesocosms. Water Res. 55, 133–142.
Wang, X., et al., 2019a. Bioconcentration, biotransformation, and thyroid endocrine disruption of decabromodiphenyl ethane (dbdpe), A novel brominated flame retardant, in zebrafish larvae. Environ. Sci. Technol. 53, 8437–8446.
Wang, Y., et al., 2019b. A comparison of the thyroid disruption induced by decabrominated diphenyl ethers (BDE-209) and decabromodiphenyl ethane (DBDPE) in rats. Ecotoxicol. Environ. Saf. 174, 224–235.
Wang, Z., et al., 2019c. Microcystin-LR exposure induced nephrotoxicity by triggering apoptosis in female zebrafish. Chemosphere 214, 598–605.
Wassarman, P.M., Litscher, E.S., 2018. The mouse egg's zona pellucida. Curr. Top. Dev. Biol. 130, 331–356.
Yanez, L.Z., et al., 2016. Human oocyte developmental potential is predicted by mechanical properties within hours after fertilization. Nat. Commun. 7, 10809.
Yu, Y., et al., 2010. Redistribution of mitochondria leads to bursts of ATP production during spontaneous mouse oocyte maturation. J. Cell. Physiol. 224, 672–680.
Zand, E., et al., 2018. Maturational gene upregulation and mitochondrial activity enhancement in mouse in vitro matured oocytes and using granulosa cell conditioned medium. Zygote 26, 366–371.
Zhang, H., et al., 2015. Multi-residue analysis of legacy POPs and emerging organic contaminants in Singapore's coastal waters using gas chromatography-triple quadrupole tandem mass spectrometry. Sci. Total Environ. 523, 219–232.
Zhang, J.W., et al., 2019. The toxic effects and possible mechanisms of glyphosate on mouse oocytes. Chemosphere 237, 124435.
Zheng, X.B., et al., 2014. Halogenated flame retardants during egg formation and chicken embryo development: maternal transfer, possible biotransformation, and tissue distribution. Environ. Toxicol. Chem. 33, 1712–1719.